Acta Crystallographica Section D
Biological Crystallography
ISSN 0907-4449

The structure of F_{420}-dependent methylenetetrahydromethanopterin dehydrogenase: a crystallographic 'superstructure' of the selenomethionine-labelled protein crystal structure

Eberhard Warkentin,[a]* Christoph H. Hagemeier,[b] Seigo Shima,[b] Rudolf K. Thauer[b] and Ulrich Ermler[a]

[a]Max-Planck-Institut für Biophysik, Marie-Curie-Strasse 15, D-60439 Frankfurt am Main, Germany, and [b]Max-Planck-Institut für Terrestrische Mikrobiologie, Karl-von-Frisch-Strasse, D-35043 Marburg, Germany

Correspondence e-mail: eberhard.warkentin@mpibp-frankfurt.mpg.de

Received 10 August 2004
Accepted 23 November 2004

PDB References: methylenetetrahydromethanopterin dehydrogenase, 1u6i, r1u6isf; 1u6j, r1u6jsf; methylenetetrahydromethanopterin dehydrogenase Se derivative, 1u6k, r1u6ksf.

The diffraction pattern of native protein crystals of F_{420}-dependent methylenetetrahydromethanopterin dehydrogenase from *Methanopyrus kandleri* shows weak additional reflections compared with the selenomethionine-labelled protein crystals, indicating a doubled *c* unit-cell parameter. These reflections indicate small reorientations of the hexameric structural units, breaking the translational symmetry. TLS refinement of the selenomethionine-labelled protein structure at 1.55 Å resolution revealed an anisotropic rigid-body libration of the hexameric units. The anisotropy is consistent with the static reorientation in the native protein crystals. These results are discussed as related to the crystal packing. The relation between the two structures suggests an analogy to structural changes during certain kinds of phase transitions that have been well studied in inorganic structural chemistry.

1. Introduction

F_{420}-dependent methylenetetrahydromethanopterin dehydrogenase (Mtd) is a protein of the methanogenic energy metabolism (Thauer, 1998). Different crystal forms have been observed for the native methylenetetrahydromethanopterin dehydrogenase from *Methanopyrus kandleri*, kMtd-nat, and the selenomethionine-labelled derivative, kMtd-Se, under the same crystallization conditions (Hagemeier, Shima, Warkentin *et al.*, 2003).

The crystal structure of kMtd-Se was solved at 1.54 Å resolution (unit-cell parameters $a = 120$, $b = 151$, $c = 110$ Å, $C222_1$) using MAD at the Se edge. The structure features trimers of dimers with local 32 D_3 (non-crystallographic) symmetry. One twofold axis of the hexamer is preserved in the crystal (Hagemeier, Shima, Thauer *et al.*, 2003). Remarkably, the pattern of the atomic displacement *B* factors in the hexamer showing the twofold (crystal) symmetry displays a striking contrast to the local 32 symmetry (Fig. 1*a*; not discussed in the previous papers).

The crystals of kMtd-nat diffracted to 2.0–2.4 Å resolution and at first sight showed the same diffraction pattern as the crystals of the selenomethionine-labelled enzyme. However, close inspection showed additional weak reflections (mean intensity ∼16% of the other reflections) along *c**, indicating a crystal structure with doubled *c* axis, $c' = 220$ Å. The apparent Laue symmetry corresponded to *mmm* ($R_{sym} = 6.1\%$; Hagemeier, Shima, Warkentin *et al.*, 2003). However, the crystal structure of kMtd-nat remained undetermined at that time.

In the following, we present the structure of the native crystals as well as a new evaluation of the kMtd-Se data using TLS refinement (Winn *et al.*, 2001).

2. Materials and methods

The sample preparation, crystallization and data collection have been described by Hagemeier, Shima, Warkentin *et al.* (2003). Diffraction data for kMtd-nat were reprocessed using *XDS* (Kabsch, 1993) and the refinement was performed with *CNS* (Brünger *et al.*, 1998) using standard scripts. Cross-validation sets from the twinned data were selected at random, assigning pairs of reflections related by the twin law to either the test or the working set using *CNS*. TLS refinement (Schomaker & Trueblood, 1968) was performed with *REFMAC*5 (Winn *et al.*, 2001). The reflection files in *CCP*4 format for kMtd-Se

were generated from the *CNS* format, preserving the cross-validation selection using the *CCP*4 program suite (Collaborative Computational Project, Number 4, 1994). The final models were evaluated with *PROCHECK* (Laskowski *et al.*, 1993) and *WHAT_CHECK* (Hooft *et al.*, 1996). Figs. 1(*a*) and 1(*b*) were generated using *MOLSCRIPT* (Kraulis, 1991) and *BOBSCRIPT* (Esnouf, 1997).

3. Results

3.1. The structure of kMtd-nat: a 'crystallographic superstructure' of the kMtd-Se crystal structure

3.1.1. The raw model. An approximate structural model for kMtd-nat, based on that of the selenomethionine-substituted protein, can be refined to R and $R_{\rm free}$ = 0.23 and 0.27 (protein only), respectively, using only the data of the small subcell of strong reflections (*i.e.* c = 110 Å, space group $C222_1$), thus accounting for roughly 86% of the total diffraction intensity. Attempts to obtain a model for the true cell (*i.e.* c = 220 Å, assuming space group $C222_1$) by molecular replacement failed [using the programs *EPMR* (Kissinger *et al.*, 1999) and *AMoRe* (Navaza, 1994)]. A unique orientation of the structural motif was always clearly found, yet no solution to the translational search could be obtained.

3.1.2. Adaptation to the true unit cell. The appearance of additional weak reflections in an otherwise largely unchanged diffraction pattern indicates a loss of translational symmetry caused by small rearrangements. An analysis of the possible low-symmetry structures (see *International Tables for Crystallography*, 1992, Vol. *A*) shows that the preservation of the 2_1 axis and the simultaneous loss of the 110 Å translation along **c** (bold type indicating a lattice vector) would enforce a tripled unit-cell parameter in this direction. This excludes space groups $C222_1$ and $P2_1$ as the symmetry of the native crystal structure. The loss of the 2_1 axis with preservation of a twofold axis in the *ab* plane, *i.e.* along either $\mathbf{a}_{\rm Se}$ or $\mathbf{b}_{\rm Se}$, would necessarily reduce the symmetry to monoclinic, resulting in either *C*211 or *C*121 (*i.e.* *C*2, which is a maximal *translationengleiche* or *t* subgroup of index 2). The two cases are termed $C2_a$ and $C2_b$, respectively, in the following. At this step of symmetry loss, the structure would have monoclinic symmetry but still the same unit cell. In a second step of symmetry loss the unit cell can be increased, again with space group *C*2 [*C*2 has again *C*2 as maximal (isomorphic) *klassengleiche* or *k* subgroup at $c' = 2c$, index 2]. Reprocessing of the diffraction data for the *C*211 case ($C2_a$) gave a = 150.9, b = 118.9, c = 219.2 Å, β = 90.0° (transformed to standard setting by $\mathbf{a}_{\rm nat} = -\mathbf{b}_{\rm Se}$, $\mathbf{b}_{\rm nat} = \mathbf{a}_{\rm Se}$, $\mathbf{c}_{\rm nat} = 2\mathbf{c}_{\rm Se}$) and for $C2_b$ a = 118.9, b = 150.9, c = 219.2 Å, β = 90.0° (with $\mathbf{a}_{\rm nat} = \mathbf{a}_{\rm Se}$, $\mathbf{b}_{\rm nat} = \mathbf{b}_{\rm Se}$, $\mathbf{c}_{\rm nat} = 2\mathbf{c}_{\rm Se}$). In both cases, $C2_a$ or $C2_b$, the new asymmetric unit contains four times as many atoms as the parent structure which is essentially preserved, however with fewer symmetry restrictions.

The merging R values ($R_{\rm sym}$ = 6.5 and 6.6%, respectively) did not make clear which of the twofold axes might have been preserved. The refinement of the models gave R and $R_{\rm free}$ values of around 37% in both cases, showing that the problem was still unsolved. Assuming the ideas developed to this point were correct, an additional factor had to be involved.

3.1.3. Twinning. An attractive hypothesis is to consider the crystals as perfectly merohedrally twinned. This would explain the good $R_{\rm sym}$ value on merging according to the *mmm* Laue class (Hagemeier, Shima, Warkentin *et al.*, 2003). Twinning is also frequently observed when a structure is formed in a *t* transition from a higher symmetry structure (Wondratschek & Jeitschko, 1976; Müller, 2004). Allowing for this twinning (*CNS*; Brünger *et al.*, 1998) decreased $R_{\rm free}$ to well below 30% on refinement in both cases, $C2_a$ and $C2_b$. The combined effect of the two twofold axes, one from the structure and one from the twinning law, prevents the distinction between the two cases in this diffraction experiment (see Table 1). The twinning operator relating

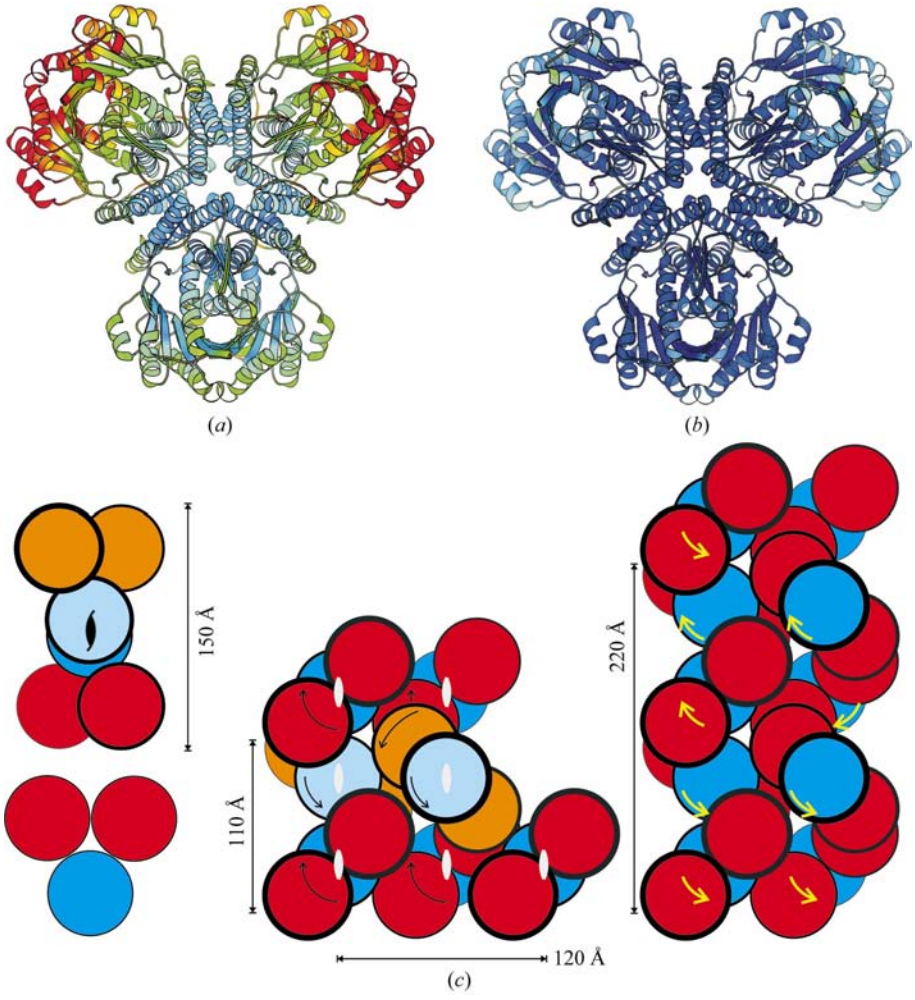

Figure 1
Illustration of the proposed flexibility of the crystal structure. (*a*) Projection of the hexameric moieties of kMtd-Se along the pseudo-threefold axis with the twofold axis ($\mathbf{b}_{\rm Se}$) vertical. The secondary structure is coloured according to the displacement factors B (blue, B = 10 Å^2; red, B = 40 Å^2). (*b*) Same as (*a*) but with B values after TLS refinement. (*c*) Bottom left, schematic view as in (*a*), with D_s in blue and D_u in red (see text); top left, two hexamers viewed along the 2_1 axis ($\mathbf{c}_{\rm Se}$) showing the overlap of the D_s dimers; middle, the packing of the hexamers in the kMtd-Se structure with sense of rotations consistent with space-group symmetry indicated by black arrows and by differing shades; right, as before for the $C2_a$ structure of kMtd-nat with yellow arrows indicating the observed sense of rotation compared with the higher symmetric parent structure (the latter two viewed along $\mathbf{b}_{\rm Se}$ and $\mathbf{a}_{\rm nat}$, respectively).

Table 1
Progress of the refinement for data set kMtd-nat1 and TLS refinement of kMtd-Se.

(*a*) kMtd-nat1.

Model	R/R_{free} $l = 2n$	All
$C222_1$	0.23/0.27	—
$C222_1$, simulated in $C2$	0.23/0.28	0.45/0.47
$C2_a$, rigid body	0.21/0.26	0.280/0.277
$C2_a$, rigid body, individual B	—	0.242/0.254
$C2_a$, protein only	—	0.203/0.252
$C2_a$ plus solvent	—	0.174/0.233
$C2_b$ with b = 150 Å	—	0.190/0.246

(*b*) kMtd-Se.

	R	R_{free}	R.m.s.d. bonds (Å)	R.m.s.d. angles (°)
CNS results	0.201	0.227	0.012	1.58
*REFMAC*5 (30–1.55 Å)	0.199	0.224	0.014	1.78
*REFMAC*5 with TLS	0.178	0.195	0.014	1.78

h, k, l to h, $-k$, $-l$ corresponds to a twofold axis in the $C222_1$ structure. In the following, only the model for case $C2_a$ with two complete (*i.e.* without any crystallographic symmetry) hexameric moieties is discussed. The $C2_b$ model features two trimers (*i.e.* two hexamers with twofold crystal symmetry) and one hexamer.

A rigid-body refinement for the $C2_a$ case starting with two hexamers from the kMtd-Se structure (see below), lowered R and R_{free} from 37% to 27.9 and 27.7%, respectively (12 parameters), and fitting of the B values lowered R and R_{free} further to 24.2 and 25.4%, respectively (see Table 1). An analogous result is obtained for the data set kMtd-nat2. A check of the refined model by *PROCHECK* showed four residues (0.1% of the non-glycine and non-proline residues) in disallowed regions of the Ramachandran plot and 27 (0.9%) in generously allowed regions.

By contrast to this apparent verification of the twin hypothesis, standard statistical tests for twinning are negative (*CNS*, following Yeates, 1997). However, when the test is applied to only the subset of weak additional reflections ($l = 2n + 1$), it indeed shows the ratio $\langle|I|^2\rangle/\langle|I|\rangle^2 = 1.49$, as expected for twinned crystals.

3.1.4. The structure. While the r.m.s. deviation between the C^α atoms of the fully refined model and the kMtd-Se structure is just 0.3 Å, the essential difference is a slight rotation (by 0.74 and 1.1°, respectively) of the two hexamers as revealed by the rigid-body refinement described above (see Table 1). This rotation is mainly composed of two contributions along the lattice vectors, a larger one around an axis close to $\mathbf{a}_{nat}$ (the molecular twofold in the $C222_1$ structure, Fig. 1) plus a smaller one around $\mathbf{c}_{nat}$ which, however, is essential in the first step of symmetry reduction. The rotations imply atomic displacements up to ∼1.5 Å far off the rotation axis. Table 2 gives the refinement statistics for data sets from two crystals.

3.2. The TLS refinement of selenomethionine-labelled kMtd

The striking contrast between the local 32 symmetry of the kMtd-Se hexamer and the twofold (crystal) symmetry of the displacement factors (Fig. 1*a*) together with the structural model obtained for kMtd-nat prompted us to re-refine the structure using the TLS model (Schomaker & Trueblood, 1968; Winn *et al.*, 2001). Remarkably, the whole asymmetric unit of kMtd-Se could be defined as one rigid group, giving a decrease in R_{free} of nearly 3% in the resolution range 30–1.55 Å (Table 3). Defining more than one rigid TLS group, for example each of the three chains or just the high-B secondary-structure segments, gave no further improvement. The overall

Table 2
Crystallographic and refinement data of Mtd from *M. kandleri*.

Values in parentheses are for the highest resolution shell. To counteract the shortage of data at this moderate resolution and owing to twinning, strong NCS restraints were imposed between the independent hexamers and weak ones to model the twofold NCS of the dimers.

	kMtd-nat1	kMtd-nat2
Space group	$C2$	$C2$
Unit-cell parameters		
a (Å)	151.0	151.3
b (Å)	119.1	119.6
c (Å)	219.3	221.1
β (°)	90.0	90.0
No. of molecules per AU	12	12
Solvent content (%)	51.7	50.8
Resolution (Å)	2.4 (2.55–2.4)	2.2 (2.4–2.2)
R_{sym} (%)	6.5 (26)	6.3 (12.3)
$I/\sigma(I)$	14.2 (5.9)	6.8 (4.8)
Completeness (%)	94.7 (89)	92.5 (86)
No. of reflections	143042	186248
Multiplicity	4.8	1.9
R_{cryst} (%)	17.4 (25.0)	18.2(26.0)
R_{free} (%)	23.3 (28.2)	23.3 (29.1)
R.m.s.d. bonds (Å)	0.007	0.007
R.m.s.d. angles (°)	1.27	1.26
Average B (Å^2)	41.1	38.0
Residues per AU	12 × 283 = 3396	12 × 283 = 3396
No. of water molecules	547	654

distribution of the displacement factors becomes more even, $B(C^\alpha)$ = 6–28 Å^2 (Fig. 1*b*) compared with $B(C^\alpha)$ = 11–66 Å^2 without TLS refinement. The average B values, with the standard deviation in

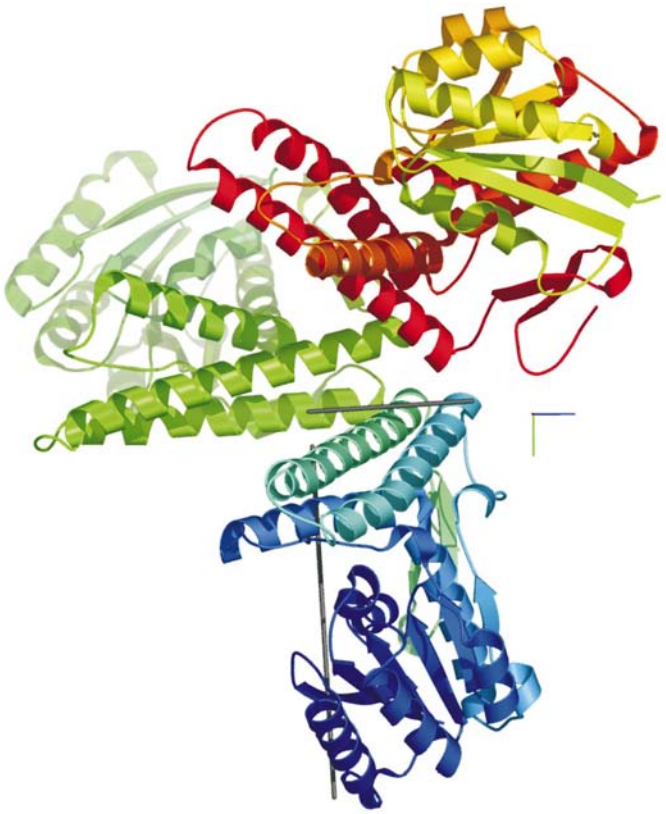

Figure 2
The non-intersecting screw axes for the TLS model for the kMtd-Se trimer. The screw axes lie parallel to the libration axes of the TLS group and the length of each is parallel to the mean-square libration around this axis. The three axes, only the longer two of which are clearly visible, are nearly parallel to the lattice vectors indicated (vertical/green, $\mathbf{b}_{Se}$; horizontal/blue, $\mathbf{c}_{Se}$; $\mathbf{a}_{Se}$ not visible). This figure was generated using *MOLSCRIPT* and *PyMol*.

parentheses, of the C^{α} atoms of the three chains are 9.8 (2.5), 11.0 (3.3) and 11.9 (4.1) Å^2 with TLS refinement and 19.4 (5.2), 27.3 (9.2) and 30.3 (12.2) Å^2 without. Thus, the treatment of the hexamer as one rigid group appears to be justified from both the *R* value and the reasonable *B* values (Fig. 1*b*). *PROCHECK* shows none of the residues in disallowed regions of the Ramachandran plot and three residues (0.5%) in generously allowed regions.

The results (see Fig. 2 and Table 3) indicate a small translational component and a markedly anisotropic behaviour for the libration, with a ratio for the main axes of 2.2:1:0.34. The mean-square libration **l** in kMtd-Se is largest around $\mathbf{b}_{Se}$ (which corresponds to the larger component of the static reorientation in kMtd-nat).

4. Discussion

4.1. Test for twinning

There is a contrast between the apparent success of the twinning hypothesis and the negative test for twinning for the whole of the kMtd-nat data. As mentioned above, the change in the kMtd-nat *versus* kMtd-Se structure gives rise to the additional 'supercell' reflections accounting for roughly 14% of the overall diffraction intensity. Thus, it seems reasonable to assume an analogously small contribution in the subset of strong 'subcell' reflections. Consistent with this assumption, the subcell intensities correspond to a reasonable approximation (see above) to a $C222_1$ model which has the twin operator as structural symmetry element (see Fig. 3). This means that for the strong subset the crystal appears not to be twinned. On the other hand, the additional 'supercell' reflections that arise from the structural change clearly indicate the twinning.

4.2. Packing analysis

These findings, the static structural change in kMtd-nat (compared with kMtd-Se) and the rigid-body libration of the hexamers in kMtd-Se, can be directly related to the packing of the hexamers. To show this, we analyse the effect of a rotation of the hexamers of the kMtd-Se structure around their twofold along $\mathbf{b}_{Se}$ (Fig. 1*c*). The dimers with twofold symmetry, D_s, within the hexamers are tightly packed along the *c* axis, having centres of gravity close to the intersection of the twofold with the screw axis along $\mathbf{c}_{se}$. Consistent with $C222_1$ symmetry, next neighbours along the screw axis will have the opposite sense of rotation and so avoid sizeable friction (like wheels in a gearbox). In the plane normal to the axis of largest libration ($\sim\mathbf{b}_{Se}$), the dimers off the twofold symmetry axis, D_u, touch the neighbouring hexamers at right angles (Fig. 1*c*), so the packing in this direction is rather invariant towards slight rotations and there would be no large steric conflict. Similar arguments hold for the D_u–D_u contacts along $\mathbf{b}_{Se}$, keeping in mind the comparatively small difference in atomic positions in the two structures.

No experiments have been performed (and would be beyond the scope of our general interest) to further clarify the cause of the growth of two different but closely related crystal forms under the same conditions (including data collection under cryoconditions) in order to determine whether this is a consequence of the selenomethionine labelling (however, no methionines were found to be involved in crystal contacts), of a deviating growth process of the organisms or of a temperature effect.

4.3. Analogy to solid–solid phase transitions

The joint occurrence of three features suggests an analogy to cases that have been well studied in inorganic structural chemistry (Wondratschek & Jeitschko, 1976; Bärnighausen, 1980; Müller, 2004): (i) two structures, with the lower symmetry one in a subgroup of the other, (ii) the rigid-body libration revealed by the TLS refinement, explaining the pattern of the displacement factors, and (iii) all crystals studied for the low-symmetry structure show a diffraction pattern with additional symmetry, *i.e.* appearing to be twinned.

In adapting the kMtd-Se structure to the larger unit cell, we had to apply two steps of symmetry reduction, the first step from $C222_1$ to *C*2, *i.e.* to a maximal *t* subgroup (*t* = *translationengleich*), the second from *C*2 to *C*2, *i.e.* to a maximal *k* subgroup (*k* = *klassengleich*; see *International Tables for Crystallography*, 1992, Vol. *A*). Both types were analysed with respect to implications for crystals undergoing a phase transition (Wondratschek & Jeitschko, 1976). *t* transitions

Table 3
Refined TLS parameters for kMtd-Se with the asymmetric unit as one rigid group.

(*a*) Elements of the **T**, **L** and **S** tensors in the orthogonal coordinate system as output by the program *REFMAC*5.

T	0.0023 0.1224 0.0818 0.0022 0.0137 0.0088
L	0.1960 1.2359 0.5923 0.0531 0.0142 0.1035
S	0.0184 −0.0102 −0.0224 −0.0656 0.0964 0.1053 0.0626 −0.0641

(*b*) Eigenvectors and eigenvalues of the reduced translation tensor in the orthogonal system.

T axis	Direction cosines			Mean-square **t** (Å^2)
1	0.999	−0.046	−0.013	−0.012
2	0.046	0.999	−0.007	0.113
3	0.013	0.006	1.000	0.049

(*c*) Orientation and position (in the orthogonal system) of the non-intersecting screw axes with the rotation and pitch of the motion about these axes.

L axis	Direction cosines			Position (Å)	Mean-square **l** (deg^2)	Pitch (Å)
1	0.999	−0.049	−0.023	61.55 64.46 25.65	0.19	−4.0
2	0.052	0.987	0.155	60.38 52.82 28.54	1.26	0.8
3	0.015	−0.156	0.988	62.32 49.14 27.30	0.58	−0.4

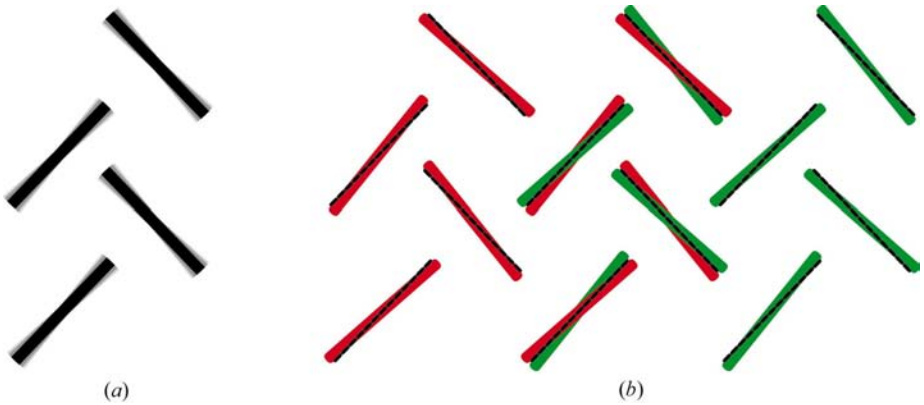

Figure 3
Twinning in the kMtd structure. (*a*) Schematic illustration of the libration around $\mathbf{b}_{Se}$ in kMtd-Se; view along $\mathbf{b}_{Se}$. (*b*) The hexamer orientation in the two twin domains is shown on the left and the right and a superposition in the middle. Black broken lines indicate the orientation in the kMtd-Se structure. For clarity, the rotation angle is increased to ±5°; view analogous to (*a*). The small rotation around *c*, essential for twin formation, is not shown.

generally give twinned crystals for the low-temperature phase. Wondratschek & Jeitschko (1976) mention as an example the Dauphiné twins of the mineral quartz that form in a *t* transition ($P6_{4/2}22$ to $P3_{1/2}21$) from the high-temperature phase. They also give an example of the two-step transition as described here.

The structural relation between the two crystal forms of factor VIII (Weiss & Hilgenfeld, 1999) is an example of the second step: a *k* transition from $P2_1$ to its isomorphous subgroup $P2_1$ with an increase in the unit cell. Another example from protein crystallography appears to be provided by the two monoclinic crystal forms of hen egg-white lysozyme (Salunke *et al.*, 1985).

Another property of *t* transitions that is of interest concerns the behaviour of vibrational modes of the crystal lattice (Scott, 1974; Shirane, 1974). One of the lattice vibration modes may soften on cooling (so-called 'soft modes'): its frequency decreases and its amplitude increases. The frequency becomes zero at the phase transition and the vibrational mode becomes a static deformation: it 'freezes out', with equal probability for the positions on either side of the former average position. Therefore, the rigid-body vibration established as a result of the TLS refinement might indicate a soft lattice-vibration mode.

We do not have enough data to postulate or directly proof the existence of a phase transition between the two kMtd-nat/kMtd-Se structures. However, the analogy to phase transitions appears to be quite obvious. So even if we were unfortunately not able to clarify the growth of two distinct crystal forms under seemingly the same conditions, it is fascinating to imagine a phase relation in a bio-crystal analogous to those in solid-state or small-molecule structural chemistry.

5. Conclusion

The crystal structure of native kMtd was shown to represent a distortion variant of the Se-labelled protein crystal structure. A re-evaluation of the kMtd-Se diffraction data using TLS refinement led to a significantly higher reliability of the structural model. The overall anisotropy of the thermal displacement factors, *i.e.* the anisotropic libration of the structural hexamers, is consistent with the change between this crystal structure and that of the native protein. The observed effects were related to the special crystal packing. The variation between the two structures is reminiscent of the structural changes during phase transitions that have been well studied in inorganic structural chemistry. The observed behaviour adds a new facet to the properties of bio-crystals and our work might contribute to the understanding and solution of thus far unrecognized similar cases.

We would like to thank H. Bärnighausen for helpful discussions and H. Michel for continuous support.

References

Bärnighausen, H. (1980). *MATCH, Commun. Math. Chem.* **9**, 139–175.
Brünger, A. T., Adams, P. D., Clore, G. M., DeLano, W. L., Gros, P., Grosse-Kunstleve, R. W., Jiang, J.-S., Kuszewski, J., Nilges, M., Pannu, N. S., Read, R. J., Rice, L. M., Simonson, T. & Warren, G. L. (1998). *Acta Cryst.* D**54**, 905–921.
Collaborative Computational Project, Number 4 (1994). *Acta Cryst.* D**50**, 760–763.
Esnouf, R. M. (1997). *J. Mol. Graph.* **15**, 132–134.
Hagemeier, C. H., Shima, S., Thauer, R. K., Bourenkov, G., Bartunik, H. D. & Ermler, U. (2003). *J. Mol. Biol.* **332**, 1047–1057.
Hagemeier, C. H., Shima, S., Warkentin, E., Thauer, R. K. & Ermler, U. (2003). *Acta Cryst.* D**59**, 1653–1655.
Hooft, R. W. W., Vriend, G., Sander, C. & Abola, E. E. (1996). *Nature (London)*, **381**, 272.
Kabsch, W. (1993). *J. Appl. Cryst.* **26**, 795–800.
Kissinger, C. R., Gehlhaar, D. K. & Fogel, D. B. (1999). *Acta Cryst.* D**55**, 484–491.
Kraulis, P. J. (1991). *J. Appl. Cryst.* **24**, 946–950.
Laskowski, R. A., MacArthur, M. W., Moss, D. S. & Thornton, J. M. (1993). *J. Appl. Cryst.* **26**, 283–291.
Müller, U. (2004). *Z. Anorg. Allg. Chem.* **630**, 1519–1537.
Navaza, J. (1994). *Acta Cryst.* A**50**, 157–163.
Salunke, D. M., Veerapandian, B., Kodandapani, R. & Vijayan, M. (1985). *Acta Cryst.* B**41**, 431–436.
Schomaker, V. & Trueblood, K. N. (1968). *Acta Cryst.* B**24**, 63–76.
Scott, J. F. (1974). *Rev. Mod. Phys.* **46**, 83–128.
Shirane, G. (1974). *Rev. Mod. Phys.* **46**, 437–449.
Thauer, R. K. (1998). *Microbiology*, **144**, 2377–2406.
Weiss, M. S. & Hilgenfeld, R. (1999). *Acta Cryst.* D**55**, 1858–1862.
Winn, M. D., Isupov, M. N. & Murshudov, G. N. (2001). *Acta Cryst.* D**57**, 122–133.
Wondratschek, H. & Jeitschko, W. (1976). *Acta Cryst.* A**32**, 664–666.
Yeates, T. O. (1997). *Methods Enzymol.* **276**, 344-358.